A Leaky-Integrate-and-Fire Neuron Analog Realized with a Mott Insulator

Pablo Stoliar, Julien Tranchant, Benoît Corraze, Etienne Janod, Marie-Paule Besland, Federico Tesler, Marcelo Rozenberg, Laurent Cario

A Leaky-Integrate-and-Fire Neuron Analogue realized with a Mott insulator

*Pablo Stoliar, Julien Tranchant, Benoit Corraze, Etienne Janod, Marie-Paule Besland Federico Tesler, Marcelo Rozenberg, and Laurent Cario**

Julien Tranchant, Benoit Corraze, Etienne Janod, Marie-Paule Besland, Laurent Cario
Institut des Matériaux Jean Rouxel (IMN), Université de Nantes, CNRS, 2 rue de la Houssinière, BP 32229,44322 Nantes Cedex 3, France
E-mail: Laurent.Cario@cnrs-imn.fr

Pablo Stoliar
CIC nanoGUNE, 20018 Donostia – San Sebastian, Basque Country, Spain

Federico Tesler
Departamento de Física-IFIBA, FCEN, Universidad de Buenos Aires, Ciudad Universitaria Pabellón I, (1428) Buenos Aires, Argentina

Marcelo Rozenberg
Laboratoire de Physique des Solides, CNRS-UMR8502, Université de Paris-Sud, Orsay 91405, France

Keywords: Leaky-integrate-and-fire, Neuron, Mott insulator

Abstract

During the last half century, the tremendous development of computers based on von Neumann architecture has led to the revolution of the information technology. However, von Neumann computers are outperformed by the mammal brain in numerous data-processing applications such as pattern recognition and data mining. Neuromorphic engineering aims to mimic brain-like behavior through the implementation of artificial neural networks based on the combination of a large number of artificial neurons massively interconnected by an even larger number of artificial synapses. In order to effectively implement artificial neural networks directly in hardware it is mandatory to develop artificial neurons and synapses. A promising advance was made in recent years with the introduction of the components called memristors that might implement synaptic functions. In contrast, the advances in artificial neurons have consisted in the implementation of silicon-based circuits. However, so far, a single component artificial neuron that would bring an improvement comparable to what memristors had brought to synapses is still missing. Here, we introduce a simple two-terminal device, which can implement the basic functions *leaky integrate and fire* of spiking neurons. Remarkably, we found that it is realized by the behavior of strongly-correlated narrow-gap Mott insulators subject to electric pulsing.

1. Introduction

During the last half century, the tremendous development of computers has led to the revolution of the information technology. Nevertheless, the way computers store and process the information has scarcely changed since their inception and relies on the concepts proposed by von Neumann in the 40's. This von Neumann architecture, based on a clear separation between the memory and the processing unit, is extremely powerful in many cases such as high-speed processing of large data streams. However, von Neumann computers are

outperformed by the mammal brain in numerous data-processing applications such as pattern recognition and data mining. [1, 2, 3, 4, 5, 6, 7, 8] In fact, the brain is organized with a very different architecture, based on a network of closely connected neurons and synapses. Neuromorphic engineering aims to mimic brain-like behavior through the implementation of artificial neural networks based on the combination of a large number of artificial neurons massively interconnected by an even larger number of artificial synapses. [2, 3] In most cases, artificial neural networks are software-implemented in conventional hardware; they are programmed in computers with standard architectures, i.e. on von Neumann architectures. In principle, a much more efficient way to that goal would be to use the so-called neuromorphic systems that allow a direct hardware implementation, that is, systems where each neuron and each synapse consists in a dedicated set of components in an electronic circuit. [4, 5]

In order to effectively implement artificial neural networks directly in hardware and integrated in high-density chips, it is mandatory to develop two types of devices: artificial neurons and synapses. [6] The key aspect here is the requirement of a vast number of these interconnected basic building blocks. Therefore any improvement in reducing the complexity, size, and power dissipation in their implementation has a huge impact on the efficiency of the whole neuromorphic system. A promising advance was made in recent years with the introduction of the components called memristors, which are highly-scalable two-terminal devices that might implement synaptic functions. [8, 9, 10] Memristors have a history dependent resistance, which may be exploited to encode a synaptic weight in a neuromorphic circuit. Moreover, they may also be integrated into high-density cross-bar arrays, which simplify the interconnection between a high number of neurons. [11] In contrast, the advances in artificial neurons have consisted in the implementation of silicon-based circuits employing many standard electronic components. A first simplification was recently achieved with the multicomponent neuristor designed with several memristors, resistances and capacitors, and

that aims to mimic the action potential of the biological neuron.[12] However, so far, a single component artificial neuron that would bring an improvement comparable to what memristors had brought to synapses is still missing.[13] Here, we introduce a simple two-terminal device, which can implement a basic function of spiking neurons, namely the *leaky integrate and fire*. Remarkably, we found that it is realized by the behavior of strongly-correlated narrow-gap Mott insulators subject to electric pulsing. [14,15,16]

2. Results and discussion

The lacunar spinel compounds AM_4Q_8 (A = Ga, Ge; M = V, Nb, Ta, Mo; Q = S, Se) containing transition-metal tetrahedral clusters are narrow gap Mott insulators with Mott-Hubbard gaps in the order of 0.1- 0.3 eV. [17] Conventional density functional calculation of the band structure yields partially filled bands, however, strong local electronic repulsion turn these materials into correlated insulators. [18] Pressure, doping or electric field can destabilize this electronic state, "melting" the Mott insulating phase into a correlated metal phase. [17,18,19,20] Both, in pressure driven or electronic doping driven insulator-to-metal transition, the physics is well accounted for by the Dynamical Mean Field Theory. [18, 21] The mechanism behind the destabilization of the Mott state upon electric field, which brings the quantum system out of equilibrium, was found recently to be related to an electronic phenomena, namely an avalanche breakdown. [14] It is not the purpose of this paper to describe the physics behind this new mechanism of resistive switching and to compare it with other mechanisms reported in the literature. These issues are addressed in recent review papers. [22] However we give hereafter a brief summary on the volatile resistive switching observed above a threshold electric field of a few kV/cm in the AM_4Q_8 compounds. Under an electric pulse exceeding the threshold electric field these narrow gap insulators undergo a dramatic resistive transition from a high to a low resistance state as described elsewhere. [14,15] This phenomenon may be observed using a simple circuit made of a two-terminal narrow-gap Mott insulator crystal

connected in series with a load resistor (see Fig. 1 (a)). Fig. 1(b) displays a typical resistive transition observed on a $GaTa_4Se_8$ sample at 74K during a voltage pulse exceeding a threshold voltage V_{th}. A sudden lowering of the voltage across the sample occurs after a (voltage dependent) delay time hereafter called t_{FIRE} *and* equal to 89 µs in this case. This lowering of the sample voltage is concomitant with an increase of the current intensity through the sample (called hereafter "*firing*" event). As a consequence, a resistive transition from a high to a low resistance state is observed (see bottom panel in Fig. 1(b)). An essential feature of this transition is that when the voltage pulse on the sample ends the sample returns to its original high resistance value after a brief delay time. This resistive transition is therefore called volatile. This volatile transition is due to the unique ability of the Mott material to locally commute between a stable insulator state and a metastable conductive state, through an electric-field driven insulator to metal transition. [15,14,20] The conductive state is characterized by metastable metallic filamentary structures bridging the electrodes and fading in time after the pulse. [16] Previous numerical modeling studies have suggested that the relaxation of the metastable metallic domains within the conducting filaments is thermally activated. [16]

To gain more understanding of this relaxation phenomenon, the evolution of the resistance after the pulse is terminated was measured and is presented in Fig. 1(c). This measurement provides the insight that the relaxation involves in fact two successive processes. Initially, right after the pulse is over, the resistance rises sharply. This may be ascribed to the filamentary conductive structure rapidly tapering itself and losing percolation. Then, once the filament is destroyed the resistance follows a long-time exponential relaxation law. This may be associated to the isolated metallic granular domains that get further reabsorbed through a thermally activated behavior as suggested by previous numerical modeling studies. [16] According to these studies, the relaxation time may be simply characterized by fitting the long time relaxation with an exponential form. Hence, we assume the form,

$$R = \left(1 - e^{-t/\tau}\right) R_0 \qquad (1)$$

which provides the satisfactory fit shown in Fig. 1(c). In Eq. (1), R_0 denotes the resistance of the pristine sample, and τ the experimental relaxation time. From the fit we can extract τ = 518 ± 100 µs. This value of τ is related to the energy barrier of the metastable metallic state, which is material dependent.

The *volatile* nature of the resistive transition described here prevents its use to implement synaptic functions like Spike-Timing-Dependent-Plasticity (STDP), which requires a *non-volatile* resistive switching as found in memristors. In contrast, the two features described above, namely a delay time t_{FIRE} and a relaxation time τ open the way to the implementation of a novel functionality "Leaky Integrate and Fire" (LIF), which realizes an analogue to a basic spiking neuron behavior. Fig. 2 illustrates this functionality. It demonstrates the spiking response of the current (*i.e.* firing) after a number of voltage pulses N_{FIRE} are applied. The main idea is to apply a train of short pulses with duration t_{ON} and separation t_{OFF} such that $t_{ON} < t_{FIRE}$ and $t_{OFF} < \tau$. For instance, in Fig. 2(a) we have t_{ON} = 20µs < t_{FIRE} = 89 µs (cf. Fig. 1(b)) and t_{OFF}=30µs < τ = 518 µs, which yields a resistive transition in the $GaTa_4Se_8$ system after N_{FIRE} = 6 pulses. The fact that the transition can be triggered with pulses of shorter duration than t_{FIRE} demonstrates that the effect is cumulative, i.e. *integrated* by the system. Moreover, Fig. 2(a) brings about the third feature of the LIF neuromorphic functionality. Indeed, the applied pulse-time elapsed until the firing (~ 6 x 20 µs) is longer than t_{FIRE} = 89 µs. This deviation from perfect integration is of course simply due to the relaxation between pulses (i.e. during t_{OFF}), which in other words realizes the *leaky* feature. Thus, N_{FIRE} depends (at a given V_{PULSE}) on the values of t_{ON} and t_{OFF}. Hence, raising t_{ON} or t_{OFF} should have opposite effects on the leaky integration and lead respectively to a decrease or an increase of N_{FIRE} which is in fact seen in Figs. 2b-c.

This “Leaky Integrate and Fire” functionality can be well understood within the framework of the model of the resistive transition in narrow-gap Mott insulators describe in details in reference [16]. To summarize, in that model the system is represented as a discretized 2D array of cells that form a resistor network (see Fig. 2). As depicted in Fig. 2(a), each cell may be in either one of two phases, which correspond to the two physical states of the system: a stable high-resistivity Mott insulator (MI) or a metastable low-resistivity correlated metal (CM). The key assumptions of the model are that the transition MI→CM can be induced by the action of a local electric field ~$q\Delta V$, with a transition rate $P_{MI\rightarrow CM} = c\, e^{-(E_B - q\Delta V)/k_B T}$, where E_B is the energy barrier with respect to the insulator state, ΔV is the voltage drop on the cell, c is a constant and q is set to unity. It is further assumed that the cells excited to the metastable state relax back thanks to a thermal activation law with a rate $P_{CM\rightarrow MI} = c\, e^{-(E_B - E_M)/k_B T}$, where E_B-E_M represents the energy barrier (see Fig. 3a).

The key quantity here $n_{CM} = N_{CM}/N$ is the ratio of the number of correlated metallic cells (N_{CM}) to the total number of cells (N). [16] Its dynamics follows

$$\frac{\partial}{\partial t} n_{CM} = -n_{CM} P_{CM\rightarrow MI} + p(t) N^{-1} \sum_{MI-cells} P_{MI\rightarrow CM} , \qquad (2)$$

where the first (loss) term account for the relaxation of CM cells back to the MI state and the second (gain) term accounts for excitation of MI cells to the CM state. Since $E_B >> k_B T$, the rate $P_{MI\rightarrow CM}$ and therefore the gain term only become significant during the voltage pulses. Hence the function $p(t)$ assumed to be $p(t)$=1 during the pulses and 0 otherwise is introduced to account for the fact that no CM sites are created without voltage. Note that while the relaxation rate $P_{CM->MI}$ is independent of the voltage on the cell, the excitation rate $P_{MI->CM}$ depends on the cell’s local drop ΔV. This introduces a strong non-linearity in the problem. The dynamical behavior can, nevertheless, be investigated in detail by numerical simulations. [16] As evidenced in reference [23] the *firing* event, i.e. the sudden growth of a filament that

percolates through the system, is found to occur when the fraction n_{CM} attains a critical value n_C. An example of the evolution of n_{CM} vs time is shown in Fig. 3(c). It is interesting to observe, that the growth of the filament occurs abruptly (compare Fig. 3(d), 3(e) and Fig. 3(f)), due to the strong non-linearity of Eq. (2). Until the *firing* event, and during the action of the applied voltage, the fraction n_{CM} increases approximately linearly in time (see Fig. 3(c)). This is because the CM cells form sparse isolated clusters ($n_{CM} << 1$), hence the electric field remains rather homogeneous through the system, yielding an almost constant production rate of CM cells, except when the number of CM cells becomes very close to the critical value n_C. There, the non-linear behavior kicks in, the production rate increases sharply and the filament percolates through the system. An important notion to realize is that for the *firing* event to occur, the production rate should dominate over the relaxation, which requires the applied voltage to be larger than a finite threshold value V_{TH}. [13] Thus, we may rewrite Eq. (2) as

$$\frac{\partial}{\partial t} n_{CM} = -n_{CM} P_{CM \to MI} + A p(t) \qquad ; V > V_{TH},\ n_{CM} < n_C \qquad (3)$$

where A is the production rate and n_C is a (model parameter dependent) critical value where the conductive filament formation suddenly occurs.

In this study we have applied this model of resistive transition to the case of train of short pulses. Importantly, Fig. 4 demonstrates that the qualitative behavior found in the case of a single pulse also occurs for application of a train of pulses, i.e., adopting a *p(t)* that subsequently switches between 1 and 0, during respective intervals t_{ON} and t_{OFF}. Specifically, during t_{ON} the CM fraction growth linearly in time (*integrate*), and during the t_{OFF} it decays exponentially in time (*leaky*). Hence, the modeling (Fig. 4) reproduces nicely the qualitative dependence of N_{FIRE} with t_{ON} and t_{OFF} as observed experimentally (Fig. 2). Moreover, it confirms that the formation of the metallic path is a sudden process occurring during a single pulse (Fig. 4d to 4g).

As we shall see below, the central result of the present work is to demonstrate that thanks to this behavior the Mott system can be considered as an analogue of a spiking neuron. Specifically, the dynamics given by Eq. (3) is analogous to the transfer function of the leaky integrate-and-fire model (LIF) of spiking neuromorphic systems. [24] These systems are a class of artificial neural networks that deal with data represented as sequences of pulses, or "spikes". The LIF model aims to describe a basic function of the neuron behavior related to the accumulation of electric charge through the cellular membrane (Fig. 4(a)). Following early work of Lapicque's, the LIF model sketched in Fig. 4(b) represents the membrane as a capacitor with a leaking resistor in parallel. [25] The increase in the membrane potential, resulting of synaptic processes (i.e., spikes arriving from other neurons) is generally modeled as current pulses that inject electrical charges into the capacitor. When the voltage reaches a given threshold the neuron fires an output electric spike. The nature of this output spike (that would represent the action potential in biological neurons) as well as the concomitant reset of the capacitor charge are usually not considered part of the model . [24, 26]

Within the LIF model of an artificial neuron that has one synaptic excitatory input-current the time dependence of the voltage *v* across the membrane is

$$\frac{\partial}{\partial t} v = -v \frac{1}{RC} + \frac{w}{C} s(t), \qquad (4)$$

with *R* the leaky resistance and *C* the capacitance of the membrane. *s(t)* represents a train of spikes arriving to the neuron. In fact, a peculiarity of the LIF model and of spiking neuromorphic systems in general, is that the information is encoded in the timing of the spikes (i.e., temporal sequence) not in their amplitude, width, etc. [14]. Furthermore, we should note that in actual neuromorphic hardware, spikes may adopt electric pulses of arbitrary shape since only their timing is relevant. The effect of the incoming spikes is controlled by the

synaptic weight *w*, which we assume a constant since the LIF model does not include the behavior of synapses.

At this stage the equivalence between the behavior of Mott insulators and the behavior of artificial neurons based on the LIF model becomes clear, as both, Eqs. (3) and (4), are analogous. Figure 5 and Table 1 summarize the equivalence between our Mott system and the LIF model. In the former, incoming spikes are represented by a train of voltage pulses and the output spike is a current pulse. As highlighted in Fig.5, a key feature of the analogy is that the role of charge accumulation in the LIF model is played in the Mott system by the accumulation of correlated metallic sites.

Finally, we illustrate the experimental validation of Eq. (3) by computing the predicted number of spikes (i.e. pulses) required to produce a *fire* event for a train with given parameters t_{ON} and t_{OFF} and applied voltage *V*. In this case, the expression for the required number of pulses N_{FIRE} can be obtained in closed form, under the simplifying assumption that the production rate of CM sites, remains constant in time (see Eq. (3)),

$$N_{FIRE} = ceiling\left(1 - \frac{\ln\left[e^{t_{OFF}/\tau} - \frac{t_{FIRE}}{t_{ON}}\left(e^{t_{OFF}/\tau} - 1\right)\right]}{t_{OFF}/\tau} \right) \quad (5)$$

Since N_{FIRE} is an integer number of pulses, we use the ceiling function which maps a real number to the smallest following integer. It is worth noting that Eq. (5) does not contain any free parameter. Both t_{FIRE} and the relaxation time τ are indeed obtained experimentally for a given fixed applied voltage. For our experimental conditions, we determined τ = 518 μs and t_{FIRE} = 89 μs (*cf* Fig. 1). Fig. 6(a) and 6(b) show the parametric dependence of N_{FIRE} with t_{ON} and t_{OFF} measured experimentally along with the theoretical prediction using Eq. (5). The

simultaneous agreement for the behavior of N_{FIRE} as a function of both, t_{ON} and t_{OFF}, provides a remarkable validation of our neuromorphic Mott device as an analogue of an artificial neuron with the LIF functionality.

3. Conclusion

We have demonstrated that the LIF neuron model can be implemented by a single component device based on a Mott insulator compound. The system implements all three basic spiking neuron processes: Leaky, Integrate and Fire. It is important to note that, this novel functionality of our Mott device goes even beyond the LIF model, as it readily implements a Firing spike by delivering an outgoing current pulse. In fact, this is one of the most complex part to implement by neuromorphic hardware. Hence, the downscaling of this simple two-terminal device may open the way for the realization of long sought after dense spiking neuromorphic networks.

In the reviewing process of our article several interesting works were published that aims to realize artificial neurons with graphene oxide [27,28] or RRAM materials [29]. All these studies fully confirm that the realization of downscalable artificial neurons will rapidly emerge as an active field of research in neuromorphic engineering.

Acknowledgements

The authors thanks the Région Pays de la Loire for funding the present work in the framework of the “Pari Scientifique Neuro-Mott” and J. Gesrel for his help in preparing the figures.

Received: ((will be filled in by the editorial staff))
Revised: ((will be filled in by the editorial staff))
Published online: ((will be filled in by the editorial staff))

Fig. 1. Experimental setup (**a**) and typical resistive switching experiments obtained on applying a long single voltage pulse (**b**). The relaxation of the resistance is shown in (**c**), and the fit of the long-time relaxation with Eq. (1) in (**d**). For the sake of the demonstration these experiments were performed at 74 K using as sample a slice of $GaTa_4Se_8$ crystal so that the resistive switching can reach almost three orders of magnitude. The inter-electrodes distances was about 40 μm which explains the large voltage needed to trigger the switching. A simple downscaling would reduce both the voltages and currents required to operate the device.

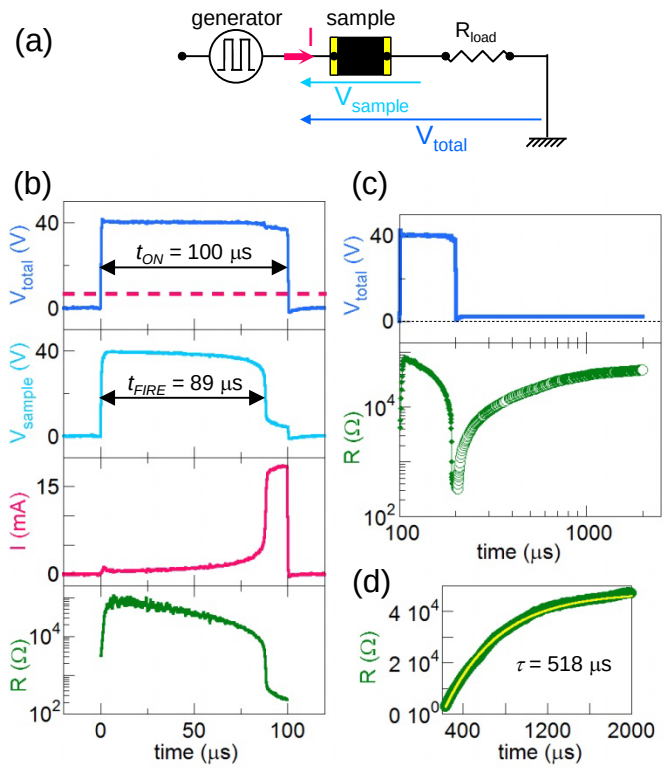

Fig. 2. Experimental resistive switching obtained by applying trains of short pulses of various t_{ON} and t_{OFF}. Using t_{ON} = 20 µs and t_{OFF} = 30 µs leads to N_{FIRE} =6 (a). Increasing t_{ON} to 30 µs leads to a decrease of N_{FIRE} to 4 (b). Increasing t_{OFF} to 80 µs leads to an increase of N_{FIRE} to 8 (c).

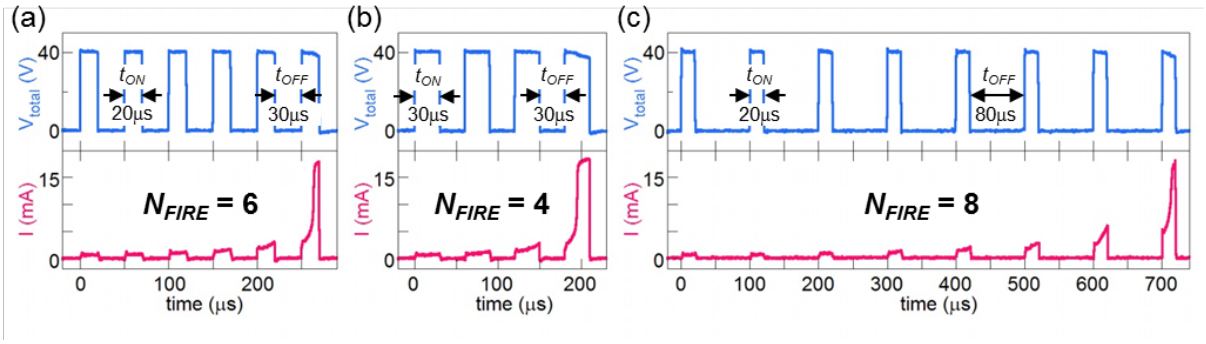

Fig. 3. Description of the energy landscape (**a**) and 2D resistor network (**b**) used for the modeling of the resistive switching in reference (16). Typical output of the model (**c**) showing before resistive switching the linear increase with time of the fraction of metallic sites. Figs. (**d**) and (**e**) display the resistance network at different time before resistive switching. A few metallic sites are created randomly. Fig. **f** shows, on the other hand, that the resistive switching is associated with the formation of a filamentary metallic path between the bottom and top electrodes.

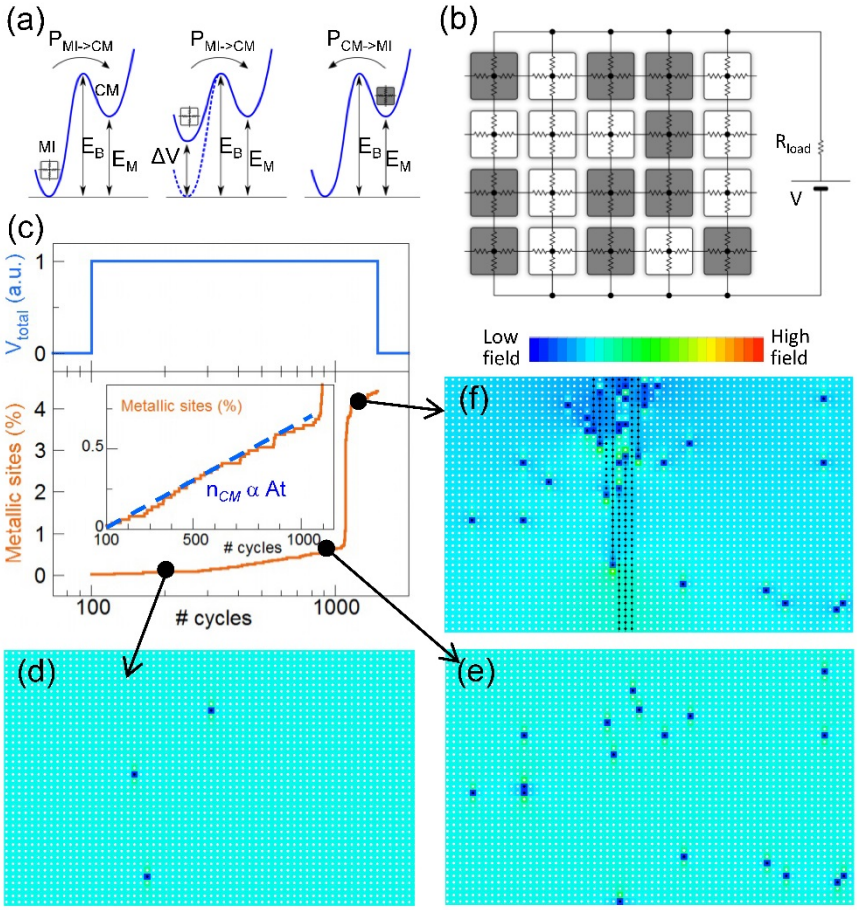

Fig. 4. Modeling of resistive switching obtained with trains of short pulses of various t_{ON} and t_{OFF} Panels (**a-c**). Panels (**d-g**) show snapshots of the microscopic state of the resistor network during each of the 4 pulses shown in panel (**a**). We observe that the formation of the conductive bridge is a sudden process, which occurs within the duration of a single pulse, i.e., in that case the fourth one.

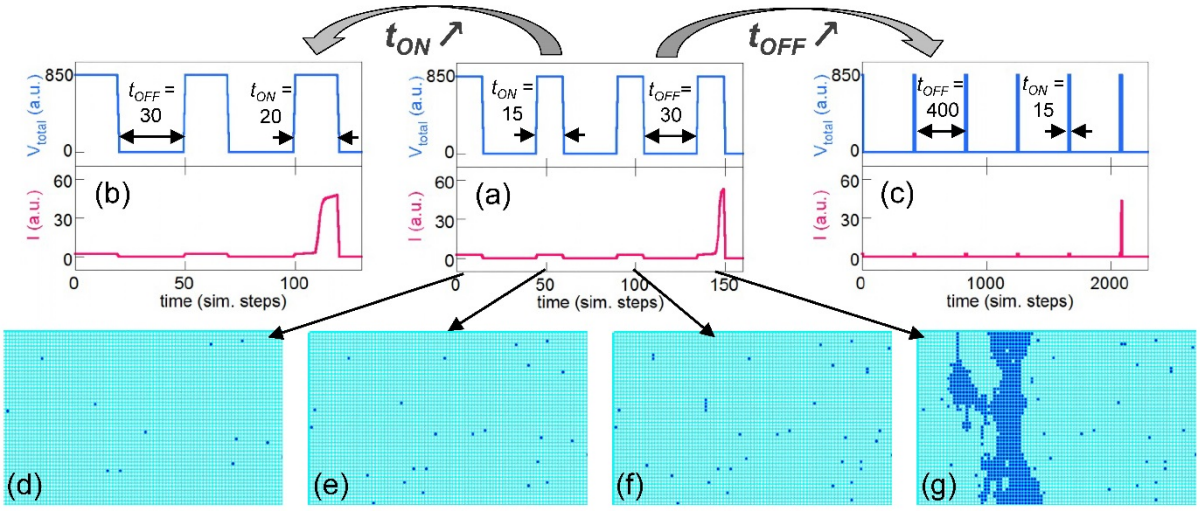

Fig. 5. Schematic representation of a biological neuron receiving input spikes from other neurons and triggering an ouput action potential when the membrane potential reaches the threshold value (**a**). The LIF artificial neurons based on Lapicque's model reproduces the evolution of the membrane potential thanks to an RC circuit accumulating electrical charges (**b**). The Mott artificial neuron sketched in (**c**) reproduces the LIF behavior thanks to the accumulation of correlated metallic sites.

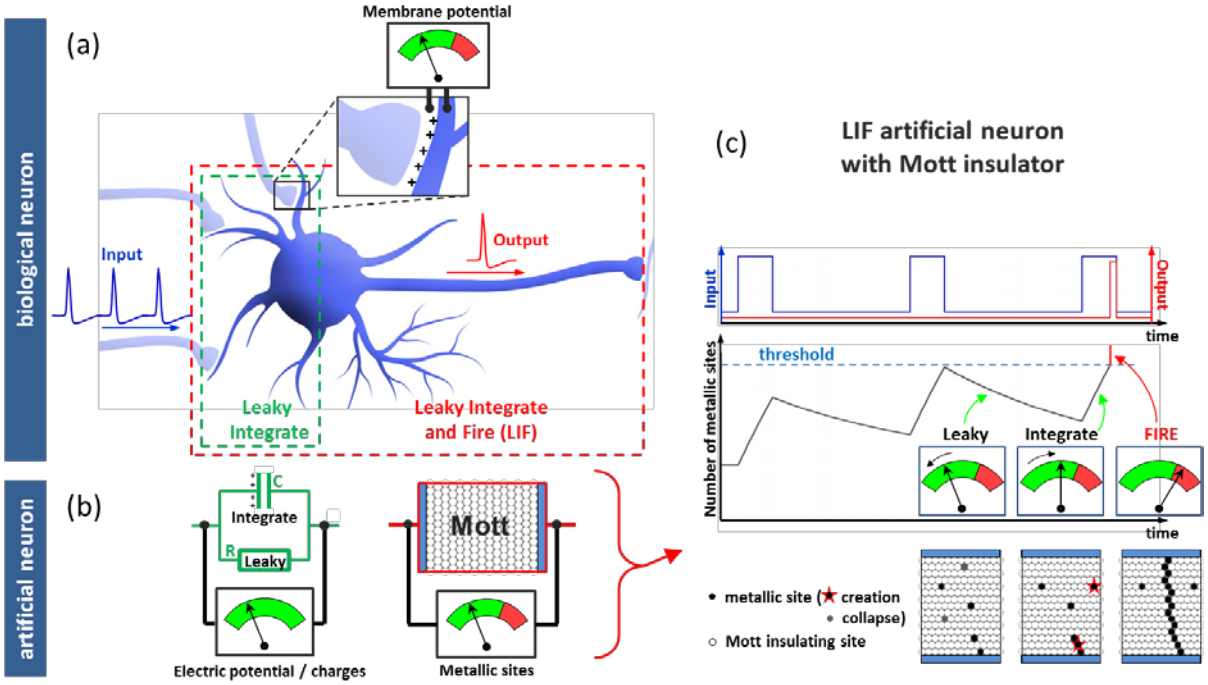

Fig. 6. Evolution of the number of pulses necessary to ″fire″ the Mott Neuron versus the pulse duration t_{ON} (a) and the separation time between pulses t_{OFF} (b). Remarkably the parameter-free theoretical prediction established for the LIF model (Eq.5, see in text), shown as red curves, reproduces nicely the experimental dependences.

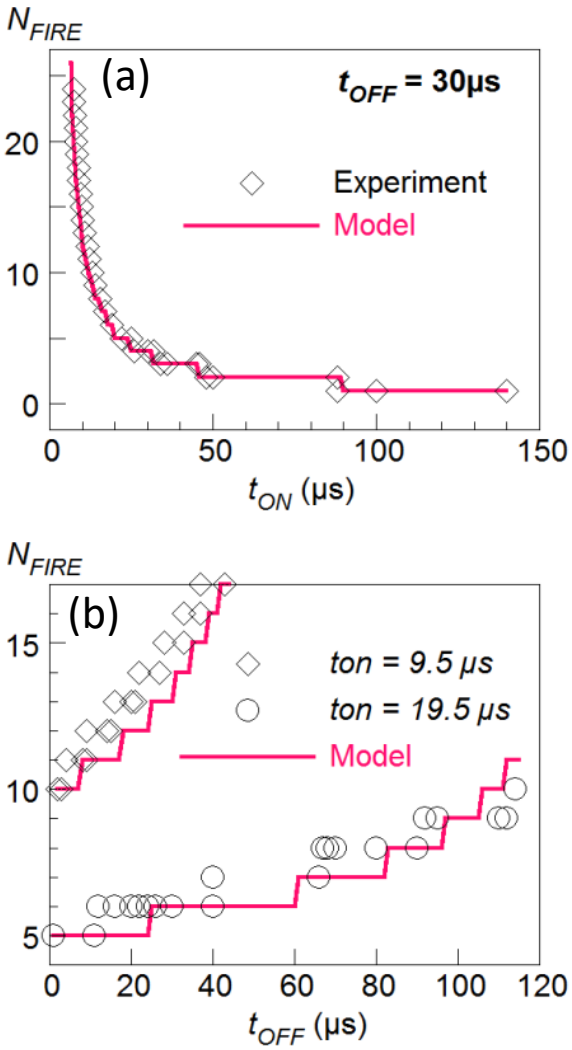

Table 1
Comparison of variables and equations used in the LIF and Mott neuron models. Both models are analogue and lead to the same equation for the number of pulse for FIRE. The ceiling function maps a real number to the smallest following integer.

	LIF model	**Mott LIF neuron**
Integrated variable	Membrane potential v	Fraction metallic regions n_{CM}
Model	$\frac{\partial}{\partial t}v = -v\frac{1}{RC} + \frac{w}{C}s(t)$	$\frac{\partial}{\partial t}n_{CM} = -n_{CM}P_{CM\to MI} + A\,p(t)$
Input variable	Dirac delta function	Voltage pulse
Output variable	Not defined	Current pulse
Leaking time-constant	RC	$1/P_{CM\to MI}$
Synaptic input	$s = \sum_i \delta(t - t_i)$	$p = \sum_i \left[H(t - t_i) - H(t - t_i - t_{ON})\right]$
Spike contribution	w/C	$A\,t_{ON}$
Number of pulses for FIRE	$N_{FIRE} = \text{ceiling}\left(1 - \frac{\ln\left[e^{t_{OFF}/\tau} - \frac{t_{FIRE}}{t_{ON}}(e^{t_{OFF}/\tau} - 1)\right]}{t_{OFF}/\tau}\right)$	

References

1. G. Indiveri, T. K. Horiuchi, *Front. Neurosci.* **2011**, *5*, 118. doi:10.3389/fnins.2011.00118.

2. C. Mead, *Proc. IEEE* **1990,** *78*, 1629.

3. A. K. Jain, J. Mao, K. M Mohiuddin, *IEEE Computer* **1996**, *29*, 31.

4. K. Boahen, Neuromorphic Microchips, *Sci. Am.* **2005,** *292*, 56.

5. J. Misra, I. Saha, *Neurocomputing* **2010**, *74*, 239.

6. C. Gao, D. Hammerstrom, *IEEE Trans. Circuits Syst. Regul. Pap.* **2007**, *54*, 2502.

7. L.P. Maguire, T.M. McGinnity, B. Glackin, A. Ghani, A. Belatreche, J. Harkin, *Neurocomputing* **2007**, ***71***, 13.

8. C. Zamarreño-Ramos, L. A. Camuñas-Mesa, J. A. Pérez-Carrasco, T. Masquelier, T. Serrano-Gotarredona, and B. Linares-Barranco, *Front. Neurosci.* **2011**, *5*, 26. doi:10.3389/fnins.2011.00026.

9. S. H. Jo, T. Chang, I. Ebong, B. B. Bhadviya, P. Mazumder and W. Lu, *Nano Lett.* **2010**, *10*, 1297.

10. D. B. Strukov, G. S. Snider, D. R. Stewart, R. S. Williams, *Nature* **2008**, ***453***, 80.

11. K.-H. Kim, S. Gaba, D. Wheeler, J. M. Cruz-Albrecht, T. Hussain, N. Srinivasa, and W. Lu, *Nano Lett.* **2012**, ***12***, 389.

[12]. M.D. Pickett, G. Medeiros-Ribeiro, R.S. Williams, *Nature Mater.* **2012**, ***12***, 114

13. G. Indiveri *et al.*, Neuromorphic Silicon Neuron Circuits, *Front. Neurosci.* **2011**, *5*, 73. doi:10.3389/fnins.2011.00073.

14. L. Cario, C. Vaju, B. Corraze, V. Guiot, E. Janod, *Adv. Mater*. **2010**, *22*, 5193.

15 V. Guiot, L. Cario, E. Janod, B. Corraze, V. Ta Phuoc, M. Rozenberg, P. Stoliar, T. Cren, D. Roditchev, *Nat. Commun.* **2013**, *4*, 1722.

16. (a) P. Stoliar, L. Cario, E. Janod, B. Corraze, C. Guillot-Deudon, S. Salmon-Bourmand, V. Guiot, J. Tranchant, M. Rozenberg, *Adv. Mater.* **2013**, *25*, 3222. (b) P. Stoliar, M. Rozenberg, E. Janod, B. Corraze, J. Tranchant, L. Cario, *Phys. Rev. B* **2014**, *90*, 045146.

17. (a) R. Pocha, D. Johrendt, B. Ni, M. M. Abd-Elmeguid, *J. Am. Chem. Soc.* **2005**, *127*, 8732. (b) M. M. Abd-Elmeguid, B. Ni, D. I. Khomskii, R. Pocha, D. Johrendt, X. Wang, K. Syassen, *Phys. Rev. Lett.* **2004**, *93***,** 126403.

18. (a) A. Camjayi, C. Acha, R. Weht, M. G. Rodríguez, B. Corraze, E. Janod, L. Cario, M. J. Rozenberg, *Phys. Rev. Lett.* 2014, *113*, 086404. (b) V. Ta Phuoc, C. Vaju, B. Corraze, R. Sopracase, A. Perucchi, C. Marini, P. Postorino, M. Chligui, S. Lupi, E. Janod, L. Cario, *Phys. Rev. Lett.* **2013**, *110*, 037401.

19. (a) E. Janod, E. Dorolti, B. Corraze, V. Guiot, S. Salmon, V. Pop, F. Christien, and L. Cario, *Chem. Mater*. **2015**, *27*, 4398. (b) E. Dorolti, L. Cario, B. Corraze, E. Janod, C. Vaju, H.-J. Koo, E. Kan, M.-H. Whangbo, *J. Am. Chem. Soc.* **2010**, 132, 5704. (c) C. Vaju, J. Martial, E. Janod, B. Corraze, V. Fernandez, L. Cario, *Chem. Mater.* **2008**, *20*, 2382.

20. (a) C. Vaju, L. Cario, B. Corraze, E. Janod, V. Dubost, T. Cren, D. Roditchev, D. Braithwaite, O. Chauvet, *Adv. Mater.s.* **2008,** *20*, 2760. (b) V. Dubost, T. Cren, C. Vaju, L. Cario, B. Corraze, E. Janod, F. Debontridder, D. Roditchev, *Nano Lett.* **2013,** *13*, 3648.

21. A. Georges, G. Kotliar, W. Krauth, M. J. Rozenberg, *Rev. Mod. Phys.* **1996**, *68*, 13.

22. (a) E. Janod, J. Tranchant, B. Corraze, M. Querré, P. Stoliar, M. Rozenberg, T. Cren, D. Roditchev, V.T. Phuoc, M.-P. Besland, and L. Cario, *Adv. Funct. Mater*. **2015**, *25*, 6287. (b) E. Janod, B. Corraze, J. Tranchant, M.-P. Besland, L. Cario, in Memristive Phenomena – From Fundamental Physics to Neuromorphic Computing **2016**, eds Rainer Waser, Matthias Wuttig, Jülich.

23. J. Tranchant, E. Janod, B. Corraze, P. Stoliar, M. Rozenberg, M.-P. Besland, L. Cario, physica status solidi (a) **2015**, *212*, 239.

24 A. N. Burkitt, *Biol. Cybern.* **2006**, 95, 97.

25 (a) L. Lapicque, *J Physiol Pathol Générale*. **1907,** *9*, 567. (b) N. Brunel, M. C. W. Rossum, *Biological Cybernetics*. **2007**, 97, 341.

26 N. Fourcaud, N. Brunel, *Neural Comput.* **2002**, *14*, 2057.

27 C. J. Wan, L. Q. Zhu, Y. H. Liu, P. Feng, Z. P. Liu, H. L. Cao, P. Xiao, Y. Shi, Q. Wan, *Adv. Mater.* **2016**, *28*, 3557.

28 C. J. Wan, Y. H. Liu, P. Feng, W. Wang, L. Q. Zhu, Z. P. Liu, Y. Shi, Q. Wan, *Adv. Mater.* **2016**, *28*, 5878.

29 A. Mehonic, A. J. Kenyon, *Front. Neurosci.* **2016**, *10*, 57.

The table of contents entry should be 50–60 words long, and the first phrase should be bold.

The mammal brain is based on a network of closely connected neurons and synapses. The implementation of artificial neural networks directly in hardware requires therefore to develop artificial neurons and synapses that can be integrated in high-density chips. Here, we demonstrate that a two-terminal device made of narrow-gap strongly-correlated Mott insulators implement the processing functions of the leaky-integrate-and-fire artificial neuron.

Keywords : Leaky-integrate-and-fire, Neuron, Mott insulator

Pablo Stoliar, Julien Tranchant, Benoit Corraze, Etienne Janod, Marie-Paule Besland Federico Tesler, Marcelo Rozenberg, and Laurent Cario*

Title : A Leaky-Integrate-and-Fire Neuron Analogue realized with a Mott insulator

ToC figure ((Please choose one size: 55 mm broad × 50 mm high or 110 mm broad × 20 mm high. Please do not use any other dimensions))